Mosaic blood vessels in tumors: Frequency of cancer cells in contact with flowing blood

Yong S. Chang*†, Emmanuelle di Tomaso*†, Donald M. McDonald‡, Rosemary Jones§, Rakesh K. Jain*, and Lance L. Munn*¶

*Steele Laboratory for Tumor Biology, Department of Radiation Oncology, and §Department of Anesthesia and Critical Care, Harvard Medical School and Massachusetts General Hospital, Boston, MA 02114; and ‡Cardiovascular Research Institute, Department of Anatomy, University of California, San Francisco, CA 94143

Edited by Stuart A. Kornfeld, Washington University School of Medicine, St. Louis, MO, and approved October 17, 2000 (received for review June 7, 2000)

The presence of ''mosaic'' vessels in which both endothelial cells and tumor cells form the luminal surface has profound implications for metastasis, drug delivery, and antivascular therapy. Yet little is known of the frequency, and thus importance, of mosaic vessels in tumors. Using CD31 and CD105 to identify endothelial cells and endogenous green fluorescent protein labeling of tumor cells, we show that ≈15% of perfused vessels of a colon carcinoma xenografted at two different sites in mice were mosaic vessels having focal regions where no CD31/CD105 immunoreactivity was detected and tumor cells appeared to contact the vessel lumen. These regions occupied ≈25% of the perimeter of the mosaic vessels, or ≈4% of the total vascular surface area in these colon carcinomas. In addition, we found similar numbers of mosaic vessels in human colon carcinoma biopsies. Our results are consistent with the observation that ≈10^6 cells are shed daily per g of tumor. More importantly, our data offer a possible explanation for the antivascular effects of cytotoxic agents and suggest potential strategies for targeting the tumor vasculature.

Many reports over the past five decades have claimed that cancer cells are located in the walls of tumor blood vessels. This idea was presented as early as 1948 (1), and ultrastructural evidence of tumor-lined vessels was reported in the 1960s by Warren and Shubik (2) and by others in the 1980s (3, 4). This issue also has been addressed in reviews on tumor blood flow (5) and in textbooks of general pathology (6). Sasaki *et al.* (7) proposed that cancer cells in these vessels might be the sites of adhesion of activated natural killer (A-NK) cells, and more recently, a controversial study by Maniotis *et al.* (8) concluded that certain uveal melanomas acquire the capability to form blood channels that are not lined by endothelial cells (9–11).

Despite these intriguing observations extending over a half-century, very little is known about the presence of tumor cells in vessel walls, and whether some examples are an artifact of the methods used to identify such cells. Other clinically significant questions include: Are blood vessels whose lumen contains tumor cells perfused? Are they unusually leaky? Do the tumor cells actively participate in forming the wall structure? Do they traverse the vessel wall? Do the exposed tumor cells increase the frequency of metastasis? Are they more susceptible to immune attack? Here, we address two of these questions—frequency and perfusion—and examine the significance of mosaic vessels in human colon cancer as well as in corresponding animal models.

To approach the problem, we first developed a technique by which cancer cells, endothelial cells, vessel morphology, and blood flow markers could be visualized simultaneously. To uniquely label cancer cells, we transfected the LS174T human colon adenocarcinoma cell line with a constitutively expressing green fluorescent protein (GFP) construct. The resulting fluorescent tumor cells then were implanted into mice and could be unambiguously identified in tissue sections.

Endothelial cells were identified by immunohistochemical labeling of tissue sections using a platelet-endothelial cell adhesion molecule (PECAM-1/CD31) and endoglin (CD105). A mixture of antibodies against CD31 and CD105 was used to increase the probability of staining all of the tumor endothelium (12, 13). To address whether the vessels under consideration were actually perfused, we injected fluorescent *Ricinus communis* agglutinin I lectin intravenously before fixing the tissue. This lectin binds weakly to the luminal surface of endothelium and strongly to the endothelial basement membrane (14, 15). These techniques were used in conjunction with three-color confocal microscopy to identify and distinguish tumor cells and endothelial cells (Fig. 1), assess three-dimensional architecture in serial confocal sections (Fig. 2), and confirm perfusion, simultaneously in a single tissue sample.

Methods

GFP Construct. To provide an endogenous marker for cancer cells, the LS174T colon carcinoma cell line was transfected with a GFP construct (driven by a constitutive promoter, EF1α). Selection was carried out by exposing the transfected cell lines to puromycin (1 μg/ml). Stable transfectants then were selected by fluorescence-activated cell sorter using a GFP filter. Finally, the resulting fluorescent cells, designated LSEFG, were implanted in the ovarian pedicle or cecal wall of female severe combined immunodeficient mice. The GFP-expressing cells were always implanted at the same passage number.

Animal Models. The GFP-expressing tumors were implanted in severe combined immunodeficient mice. To assess the effect of the host microenvironment on the cellular composition of vessels, the fluorescent tumor cells were implanted at two different sites: the ovarian pedicle and the cecum. The ovarian pedicle implantation allows the study of the newly formed tumor vessels in an ectopic location (16) whereas the cecum provides an orthotopic environment for tumor growth. In the ectopic model, a tumor chunk was implanted in the ovarian pedicle after ovariectomy and allowed to grow to 6–10 mm over a period of 10–14 days (16). Contact between the tumor and surrounding tissue was prevented by enclosing the tumor in a Parafilm bag. Consequently, the tumor developed its own blood supply, allowing the study of the resulting new angio-

This paper was submitted directly (Track II) to the PNAS office.

Abbreviation: GFP, green fluorescent protein.

†Y.S.C. and E.d.T. contributed equally to this work.

¶To whom reprint requests should be addressed at: Harvard Medical School and Massachusetts General Hospital, Department of Radiation Oncology, 100 Blossom Street, Cox-7, Boston, MA 02114. E-mail: lance@steele.mgh.harvard.edu.

The publication costs of this article were defrayed in part by page charge payment. This article must therefore be hereby marked "*advertisement*" in accordance with 18 U.S.C. §1734 solely to indicate this fact.

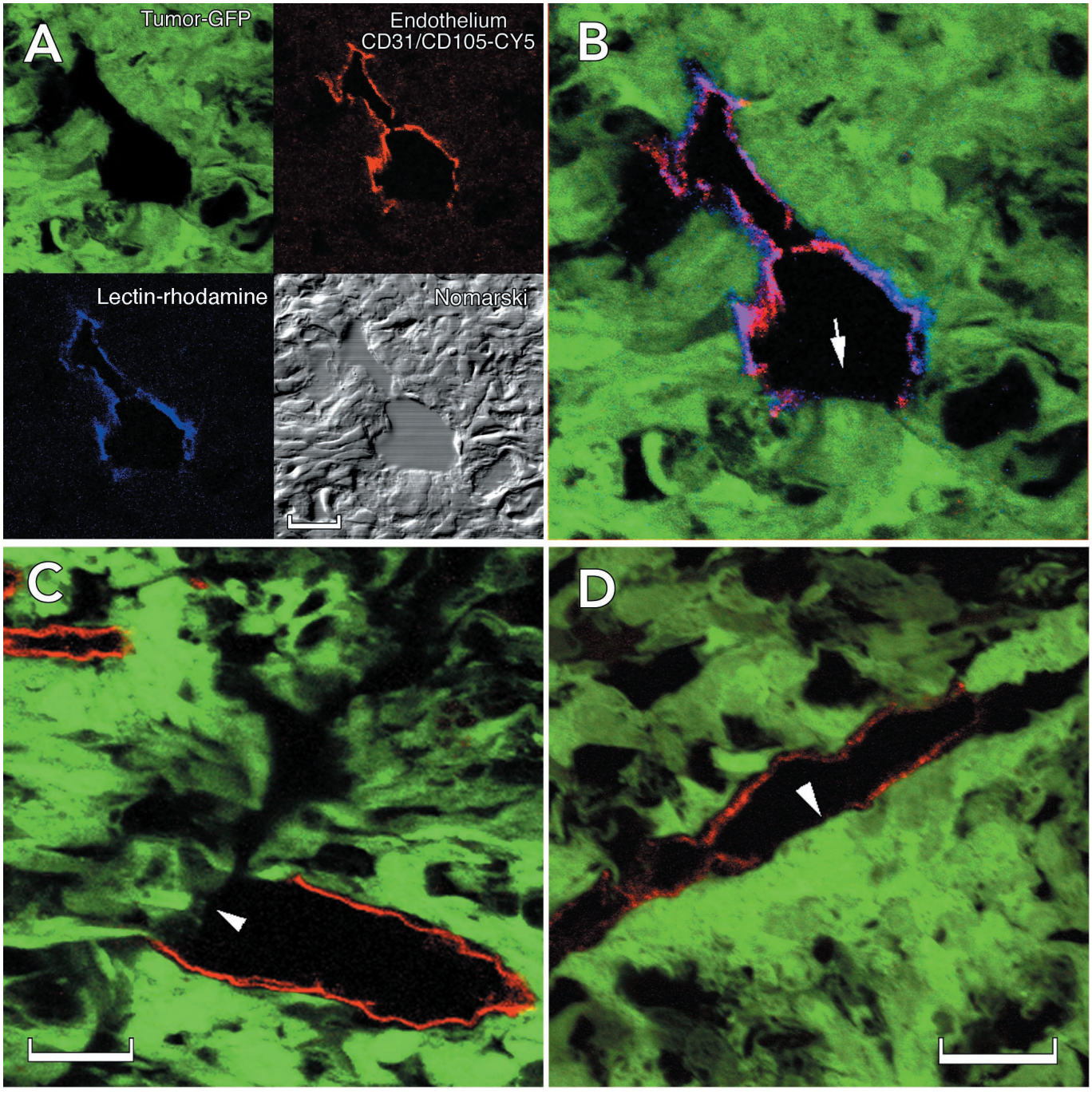

Fig. 1. Identification of cellular constituents of the vascular wall in LS174T tumor xenografts. (*A*) Summary of the method used to identify mosaic vessels. Endogenous GFP expression by the implanted tumor cells (green) along with lectin fluorescence to mark perfused vessels (blue, rhodamine pseudocolor) and CD31/CD105 immunostaining (red, Cy5) for endothelium defines the cellular composition of the tumor vessels. (*B*) Composite three-color representation of the vessel in *A*. (*C* and *D*) Individual confocal slices (1 μm) from the orthotopic (*C*) and the ectopic tumors (*D*) showing apparent tumor cell involvement in the wall. The lectin staining has been omitted for clarity. Arrows mark regions that lack detectable CD31/CD105 immunoreactivity. (Scale bar: *A* and *C*, 20 μm; *D*, 50 μm.)

genic vessels. For the orthotopic tumor model, after a midline incision into the abdominal cavity, a fine-line nick was made on the serosa layer of the cecum, and 0.5- to 1-mm LSEFG tumor chunks were sutured into a pocket in the cecal wall. The resulting tumors reached a size of 3–5 mm.

Perfusion Fixation. Tumors were fixed by vascular perfusion of 4% paraformaldehyde in PBS. After opening of the thorax, a blunt 18-gauge needle was inserted into the left ventricle of the heart of anesthetized mice. Once the auricles of both atria were opened, 4% paraformaldehyde was perfused through the mouse vasculature at 120 mmHg pressure (17).

Lectin Perfusion. To address whether the vessels under consideration were actually functional blood vessels, we injected rhodamine-labeled *Ricinus communis* agglutinin I (15) lectin (Vector Laboratories) as a marker of the blood perfusion. The lectin was injected systemically at 10 μl/g of body weight 5 min

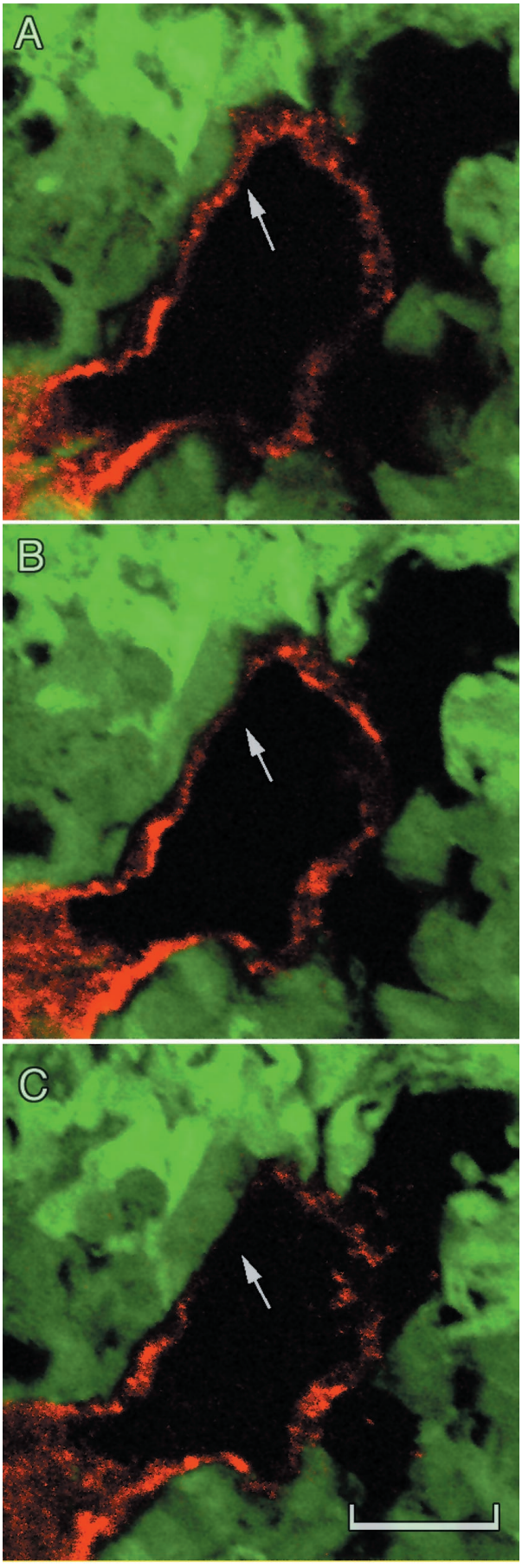

before fixation. Using this technique, we found no evidence of nonperfused mosaic vessels (17).

Immunohistochemistry. For each tumor xenograft, 3- to 10-μm thick cryo-sections were cut from varying depths of tumor. A mixture of rat anti-mouse CD31 and rat anti-mouse CD105 (PharMingen) was used at 1/250 dilution overnight at 4°C. Cy5-labeled donkey anti-rat (1/400 dilution, Jackson Immunoresearch) was incubated for 3 h at room temperature for visualization. For human tumors, paraffin sections (5 μm) were stained by using Dako Envision double-stain system. Mouse anti-human CD31 (clone JC/70A Dako) and mouse anti-human CD105 (Endoglin SN6h Dako) were used to visualize endothelial cells, and rabbit anti-human carcinoembryonic antigen (Dako) to visualize tumors cells. Incubation times and dilutions were according to the manufacturer's protocol.

Quantification. Optical images were obtained by using a Leica TCS-NT 4D confocal microscope from nine ectopic and five orthotopic tumors. Tumor cells were identified by their endogenous expression of GFP (excitation 488 nm), and endothelial cells by labeling the two endothelial cell markers (CD31 and CD105) with Cy5 (excitation 633 nm). Captured images then were transferred and quantified by using the National Institutes of Health IMAGE software (public domain software; available at http://RSB.info.NIH.gov/NIH-image/). Vessel diameters were measured as the minimum axis of the best fit-ellipse to the lumen. Rarely (less than ≈2%), the vessel wall was not completely labeled with green (tumor cell) or red (endothelial cell) fluorescence. In these cases, it is possible that another cell type (e.g., fibroblast, pericyte, or circulating cell) participated in the structural makeup of these vessels. It is also possible, however, that they were endothelial cells that expressed neither CD31 nor CD105 or tumor cells that had lost GFP expression.

Results

For quantification, mosaic vessels were defined as blood vessels with GFP-expressing tumor cells in apparent contact with the lumen, as indicated by the absence of detectable overlying CD31/CD105 immunoreactivity. These vessels had a discontinuity in the CD31/CD105-stained endothelium, and GFP-expressing cells were located in the unstained region. From a total of 947 vessels examined in nine ectopic (ovarian pedicle site) tumors, 130 were mosaic vessels (13.7%). In these nine tumors, the occurrence of mosaic vessels ranged from 8% to 22%, and in five of nine tumors it fell between 14% and 16% (Table 1). These numbers were not significantly different from those obtained for the orthotopic (cecum) tumors ($P > 0.45$), where 15.6% of the 608 vessels examined had mosaic walls. This result suggests that the location of colon carcinoma growth does not affect the frequency of mosaic vessel occurrence.

In general, vessel diameters in the ectopic tumors were smaller than those in orthotopic tumors. The mean diameters for "endothelial" (i.e., with continuous CD31/CD105 staining) and mosaic vessels were 10.5 ± 7.2 μm and 10.7 ± 4.4 μm, respectively in the ectopic site and 19.8 ± 15.3 μm and 23.0 ± 8.22 μm, respectively in the orthotopic site (Table 1). The difference between orthotopic and ectopic mosaic vessel diameters was significant ($P < 0.03$), but no significant correlation between vessel diameter and the percentage of mosaic vessels was seen. Only perfused vessels, as judged by the colocalization of lectin

Fig. 2. Confocal slices from three different depths within one of the orthotopic tumors. *C* shows a region where the red CD31/CD105 immunoreactivity is no longer visible. (Scale bar, 20 μm; depth between each section, 2.5 μm.)

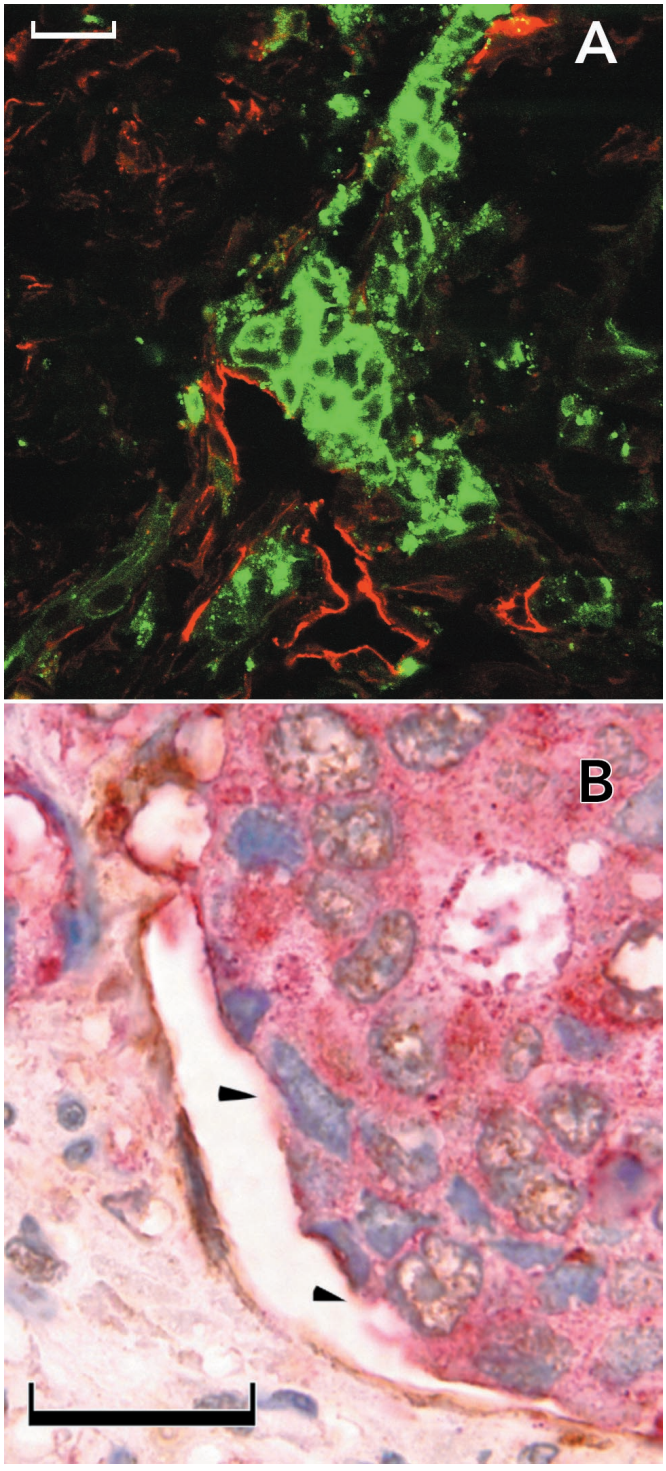

Fig. 3. Mosaic vessels in human colon cancer. (*A*) Fluorescence confocal image of double-staining with anti-CD31 (visualized with Texas red), anticarcinoembryonic antigen (visualized with FITC). Arrowhead marks a region lacking detectable CD31 immunoreactivity. (*B*) Bright-field double-staining with anti-CD31 (visualized with diaminobenzidine), anticarcinoembryonic antigen (visualized with fast-red), and hematoxylin. (Scale bars: 50 μm.)

staining and CD31/CD105 labeling, were included in the analysis. Stagnant blood "lakes" were not labeled by the lectin and therefore were excluded.

Platelets were apparently adherent to some cancer cells in contact with the vessel lumen, but no thrombi were seen (data not shown). Vessels considered in the analyses were located within the tumor mass, and cancer cells with no overlying CD31/CD105 staining were in contact with other cancer cells (Fig. 1*C*). The percentage of vessel perimeter lacking CD31/CD105 staining varied greatly from vessel to vessel. On average, 21.6 ± 6.4% (ectopic) and 25.9 ± 7.2% (orthotopic) of the perimeter of the mosaic vessels lacked CD31/CD105 staining; the corresponding ranges were 4% to 75% (ectopic) and 3% to 64% (orthotopic). Based on these values, the regions lacking CD31/CD105 immunoreactivity averaged an estimated 7 μm in ectopic tumors and 19 μm in orthotopic tumors. From the product of the mean proportion of mosaic vessels and the mean length of vessel perimeter unstained with the endothelial markers, approximately 4% of the total vessel luminal surface area was not stained with either CD31 or CD105.

A selected array of human biopsies of colon carcinoma showed mosaicism similar to that seen in the xenografts (Fig. 3). The 16 human tumors ranged from highly differentiated, lobular tumors with vessels located in stromal tissue separating tumor glandular structures to poorly differentiated masses with vessels randomly distributed throughout. In agreement with our animal model data, 13.6% of the 367 vessels studied were mosaic. In the 16 tumors quantified, the frequency of mosaic vessels was unrelated to the tumor grade/stage.

Discussion

The unusual properties of tumor vasculature have been the subject of much research, ranging from analyses of the endothelial cell junctions (17, 18) to analyses of the chaotic network branching patterns (19). The endothelial cells of tumor vessels can be highly attenuated and abnormal, as determined by electron microscopy (4, 17). In light of these observations, tumor endothelial cells may differ from those of normal tissue with respect to platelet-endothelial cell adhesion molecule 1 and endoglin expression. In this study, we have used rigorous techniques to identify mosaic vessels as defined by regions lacking CD31/CD105 immunoreactivity. However, it is possible that the tumor environment produces endothelial cells that have insufficient CD31 and CD105 immunoreactivity to be identified with these methods. Further studies that involve transmission electron microscopy or combine immunostaining with electron microscopy are needed to resolve this issue.

Although the number of mosaic vessels identified in this study appears high, other published data are consistent with our conclusions. For example, it has been shown that approximately one million cells are shed per g of tumor per day (20, 21). This number also has been confirmed in LS174T tumors grown in the ovarian pedicle (22). We also know that the vascular surface area of the LS174T tumor is approximately 370 cm^2/cm^3 (23). Combining these numbers with our mosaic data, we obtained the plausible result that approximately half of the tumor cells in contact with the vessel lumen would be shed in a given day. This calculation assumes a vessel length density per area of 190 cm/cm^2 taken with an optical depth of focus of 24 μm (23). The average vessel diameter was assumed to be 15 μm (23) and the area of cell exposure 30 μm^2 per cell. The calculation assumes that all tumor cells in contact with the vessel lumen are in the process of intravasation, which may not be the case.

Other evidence that fits our hypothesis comes from studies of lymphocyte adhesion that show preferential adhesion of activated natural killer (A-NK) cells in tumors (7, 24, 25). It is intriguing that a high level of adhesion occurs in only 10% of the vessels (24). Our results are consistent with the hypothesis that these A-NK cells bind to the luminally exposed tumor cells, as the number of mosaic vessels in the examined tumors is on the order of 10%.

A comparison of our findings with functional and ultrastructural studies of vascular permeability raises questions about the

Table 1. Quantification of mosaic vessels and their characteristics

Tumor	Total no. of vessels	No. of mosaic		% mosaic	Tumor cell lining, %	Mosaic vessel diameter,* μm
Ectopic (ovarian pedicle)						
1	282	41		14.54	19.03	10.90
2	113	18		15.93	19.74	15.67
3	34	5		14.71	11.07	5.61
4	67	15		22.39	19.26	19.35
5	131	11		8.40	17.40	11.51
6	39	3		7.69	19.87	10.48
7	91	14		15.38	28.62	8.60
8	90	13		14.44	30.30	8.56
9	100	10		10.00	28.79	5.92
Total	947	130	Mean	13.72	21.56	10.73
			SD	4.52	6.36	4.44
Orthotopic (cecum)						
1	190	25		13.16	17.33	26.55
2	98	22		22.45	20.69	30.09
3	128	17		13.28	25.33	19.87
4	148	16		10.81	34.72	10.08
5	44	8		18.18	31.41	28.51
Total	608	88	Mean	15.58	25.90	23.02
			SD	4.69	7.23	8.22

*Diameter refers to luminal diameter.

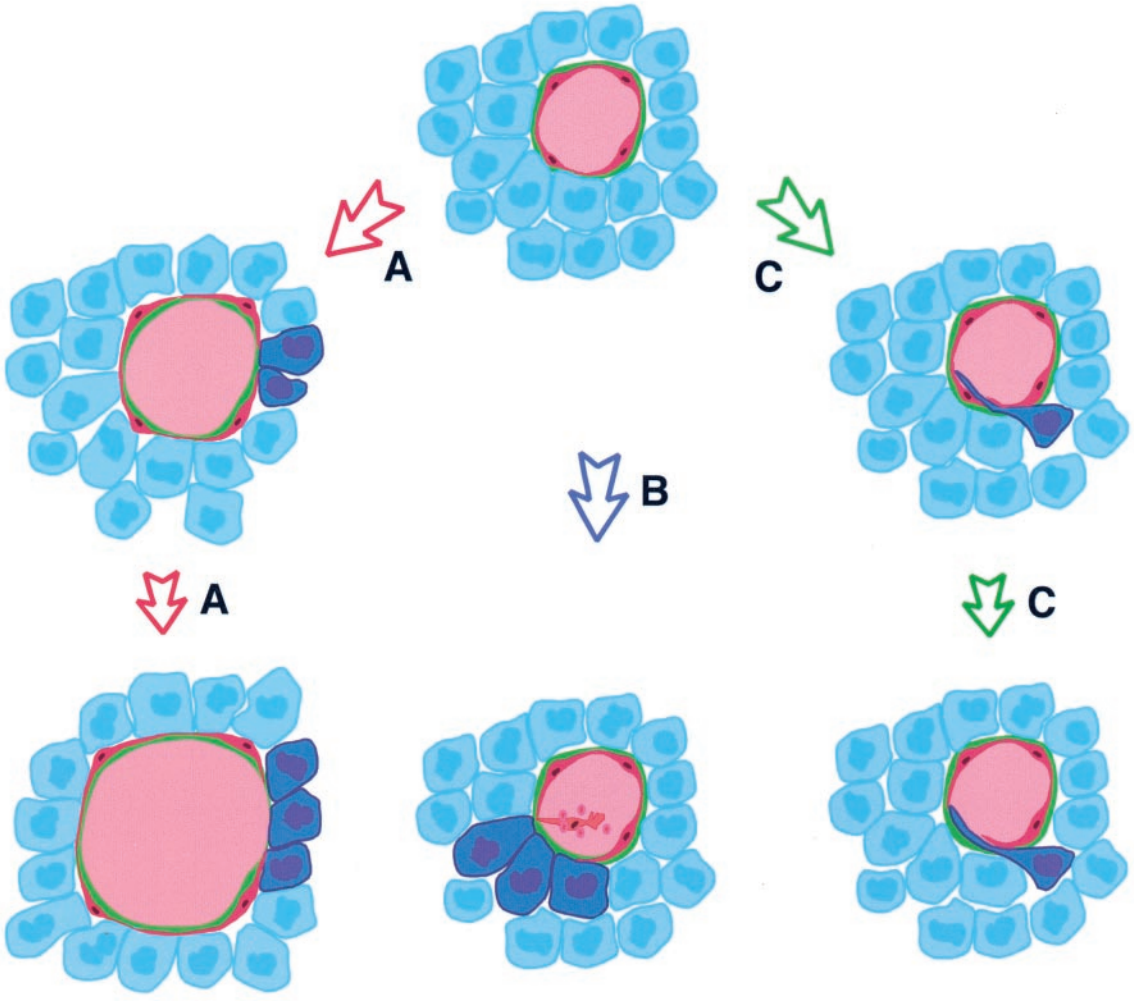

Fig. 4. Potential mechanisms of mosaic vessel formation (endothelial cells: red; cancer cells: blue). In *A*, rapid vessel growth occurs via endothelial migration without sufficient endothelial proliferation, leaving cancer cells (dark blue) exposed to the lumen. In *B*, an endothelial cell (red) is shed from the lining, exposing underlying tumor cell(s). In *C*, a tumor cell (dark blue) invades the vessel, displacing an endothelial cell that may later be lost from the lining. Our morphological data are most consistent with *B*.

interface between the cancer and endothelial cells. Titrations of liposome extravasation in the LS174T tumor revealed a pore size range of 400 to 600 nm (26). These functional findings were supported by electron microscopic evidence of endothelial defects of similar size (17). However, these transport pathways are much smaller than the apparent areas of cancer cell exposure in mosaic vessels ($\approx$10–25 μm). Thus, further experiments are needed to determine whether endothelial cells that lack CD31/CD105 immunoreactivity participate in the barrier or whether the extracellular matrix and tumor cell–endothelial cell interfaces restrict transport in these mosaic vessels.

Finally, our results may shed light on some preclinical studies that have shown impressive antitumor responses. The antivascular effects of some anticancer therapies could be explained by mosaic vessels, because killing exposed cancer cells could impair blood flow in 14% of the vessels causing significant antivascular effects (27–32). This does not exclude the possibility that anticancer drugs have direct antiendothelial effects.

This study has demonstrated that mosaic vessels are, indeed, abundant in human tumors and animal models, but how are these vessels formed? Perhaps some endothelial cells loose the CD31/105 immunoreactivity and thereby become invisible in our system. Alternatively the cancer cells may become exposed to the lumen upon the shedding of existing endothelial cells (Fig. 4*B*). If tumor vessel formation is rapid and haphazard, and endothelial proliferation is insufficient or endothelial junctions are unstable, perhaps cancer cells are temporarily exposed and participate in vessel walls (Fig. 4*A*). It should be emphasized that the tumor cells in apparent contact with the lumen do not show an endothelial phenotype (Fig. 4*C*) as they do not have CD31/CD105 immunoreactivity or the shape of endothelial cells. Therefore, the formation of mosaic vessels identified in this study is distinct from vasculogenic mimicry as described by Maniotis *et al*. (8).

Physiologically, an imbalance in the growth factors responsible for tumor angiogenesis, including vascular endothelial growth factors, basic fibroblast growth factor, angiopoietins, and ephrins, may be disruptive enough to disorient the angiogenic endothelial cells, resulting in mosaic vessels. And as for the implications for tumor vascularization, it is possible that circulating endothelial precursor cells (33–35) could later cover the exposed tumor cells, incorporating into the vessel wall and facilitating angiogenesis.

Because CD31/CD105-labeled debris resembling apoptotic bodies was occasionally seen near the mosaic regions (data not shown) it is possible that, during the process of angiogenesis or vascular co-option, endothelial cells surrounded or displaced by cancer cells are lost through apoptosis (35). Only further investigation will resolve these questions. In the meantime our findings provide quantitative data on mosaic vessels in tumors and have potential implications for vascular targeting and cancer therapy (35).

We thank Sybill Patan for her work in the initial stage of the study; Yves Boucher for scientific input on morphology and immunohistochemistry; Sylvie Roberge for her help with the tumor implantations; Takeshi Gohongi for his help with the orthotopic tumor implantations; Yi Chen and Brian Seed for the LSEFG cells; Peter Baluk and Shunichi Morikawa for help with the perfusion fixation and lectin labeling procedures; and Carolyn Compton for providing the human biopsies. This work was supported by National Institutes of Health Grants R35 CA 56591 (to R.K.J.), PO1 CA80124 (to R.K.J. and L.L.M.), T32 CA-73479 (to Y.S.C.), and HL24136 (to D.M.M.) and a grant from the Whitaker Foundation (to L.L.M.).

1. Willis, R. A. (1948) *Pathology of Tumours* (Butterworth, London).
2. Warren, B. A. & Shubik, P. (1966) *Lab. Invest.* **15,** 464–478.
3. Prause, J. U. & Jensen, O. A. (1980) *Albrecht Von Graefes Arch. Klin. Exp. Ophthalmol.* **212,** 261–270.
4. Hammersen, F., Endrich, B. & Messmer, K. (1985) *Int. J. Microcirc. Clin. Exp.* **4,** 31–43.
5. Jain, R. K. (1988) *Cancer Res.* **48,** 2641–2658.
6. Majno, G. & Joris, I. (1996) *Cells, Tissues, and Disease: Principles of General Pathology* (Blackwell, Cambridge, MA).
7. Sasaki, A., Melder, R. J., Whiteside, T. L., Herberman, R. B. & Jain, R. K. (1991) *J. Natl. Cancer Inst.* **83,** 433–437.
8. Maniotis, A. J., Folberg, R., Hess, A., Seftor, E. A., Gardner, L. M., Pe'er, J., Trent, J. M., Meltzer, P. S. & Hendrix, M. J. (1999) *Am. J. Pathol.* **155,** 739–752.
9. Barinaga, M. (1999) *Science* **285,** 1475.
10. Bissell, M. J. (1999) *Am. J. Pathol.* **155,** 675–679.
11. McDonald, D. M., Munn, L. & Jain, R. K. (2000) *Am. J. Pathol.* **156,** 383–388.
12. Seon, B. K., Matsuno, F., Haruta, Y., Kondo, M. & Barcos, M. (1997) *Clin. Cancer Res.* **3,** 1031–1044.
13. Kumar, S., Ghellal, A., Li, C., Byrne, G., Haboubi, N., Wang, J. M. & Bundred, N. (1999) *Cancer Res.* **59,** 856–861.
14. Wadsworth, J. D., Okuno, A. & Strong, P. N. (1993) *Biochem. J.* **295,** 537–541.
15. Thurston, G., Baluk, P., Hirata, A. & McDonald, D. M. (1996) *Am. J. Physiol.* **271,** H2547–H25462.
16. Kristjansen, P. E., Roberge, S., Lee, I. & Jain, R. K. (1994) *Microvasc. Res.* **48,** 389–402.
17. Hashizume, H., Baluk, P., Morikawa, S., McLean, J., Thurston, G., Roberge, S., Jain, R. K. & McDonald, D. M. (2000) *Am. J. Pathol.* **156,** 1363–1380.
18. Roberts, W. G. & Palade, G. E. (1997) *Cancer Res.* **57,** 765–772.
19. Baish, J. W. & Jain, R. K. (2000) *Cancer Res.* **60,** 3683–3688.
20. Liotta, L. A., Kleinerman, J. & Saidel, G. M. (1974) *Cancer Res.* **34,** 997–1004.
21. Butler, T. P. & Gullino, P. M. (1975) *Cancer Res.* **35,** 512–516.
22. Swartz, M. A., Kristensen, C. A., Melder, R. J., Roberge, S., Calautti, E., Fukumura, D. & Jain, R. K. (1999) *Br. J. Cancer.* **81,** 756–759.
23. Leunig, M., Yuan, F., Menger, M. D., Boucher, Y., Goetz, A. E., Messmer, K. & Jain, R. K. (1992) *Cancer Res.* **52,** 6553–6560.
24. Melder, R. J., Salehi, H. A. & Jain, R. K. (1995) *Microvasc. Res.* **50,** 35–44.
25. Melder, R. J., Koenig, G. C., Witwer, B. P., Safabakhsh, N., Munn, L. L. & Jain, R. K. (1996) *Nat. Med.* **2,** 992–997.
26. Hobbs, S. K., Monsky, W. L., Yuan, F., Roberts, W. G., Griffith, L., Torchilin, V. P. & Jain, R. K. (1998) *Proc. Natl. Acad. Sci. USA* **95,** 4507–4512.
27. Senter, P. D., Saulnier, M. G., Schreiber, G. J., Hirschberg, D. L., Brown, J. P., Hellstrom, I. & Hellstrom, K. E. (1988) *Proc. Natl. Acad. Sci. USA* **85,** 4842–4846.
28. Trail, P. A., Willner, D., Lasch, S. J., Henderson, A. J., Hofstead, S., Casazza, A. M., Firestone, R. A., Hellstrom, I. & Hellstrom, K. E. (1993) *Science* **261,** 212–215.
29. Huang, X., Molema, G., King, S., Watkins, L., Edgington, T. S. & Thorpe, P. E. (1997) *Science* **275,** 547–550.
30. Jain, R. K., Safabakhsh, N., Sckell, A., Chen, Y., Jiang, P., Benjamin, L., Yuan, F. & Keshet, E. (1998) *Proc. Natl. Acad. Sci. USA* **95,** 10820–10825.
31. Browder, T., Butterfield, C. E., Kraling, B. M., Shi, B., Marshall, B., O'Reilly, M. S. & Folkman, J. (2000) *Cancer Res.* **60,** 1878–1888.
32. Klement, G., Baruchel, S., Rak, J., Man, S., Clark, K., Hicklin, D., Bohlen, P. & Kerbel, R. (2000) *J. Clin. Invest.* **105,** R15–R24.
33. Asahara, T., Murohara, T., Sullivan, A., Silver, M., van der Zee, R., Li, T., Witzenbichler, B., Schatteman, G. & Isner, J. M. (1997) *Science* **275,** 964–967.
34. Rafii, S. (2000) *J. Clin. Invest.* **105,** 17–19.
35. Carmeliet, P. & Jain, R. K. (2000) *Nature (London)* **407,** 250–257.